AJNR

Phase-contrast imaging of the parotid region.

D J Mikulis, R Chisin, G L Wismer, R B Buxton, A L Weber, K R Davis and B Rosen

Phase-Contrast Imaging of the Parotid Region

David J. Mikulis[1]
Roland Chisin[1]
Gary L. Wismer[1]
Richard B. Buxton[1]
Alfred L. Weber[2]
Kenneth R. Davis[1]
Bruce Rosen[1]

Standard T1- and T2-weighted spin-echo acquisitions were compared with T1- and T2-weighted phase-contrast techniques in a series of 10 consecutive patients with parotid masses to assess the role of phase-contrast methods in the evaluation of lesions in the parotid fossa. Greater tissue-lesion contrast was obtained with phase-contrast methods in nine of 10 cases, allowing improved lesion visualization; however, an increase in lesion detectability was not observed in this series. Standard MR imaging methods are sufficient for imaging the parotid region in most cases, but can be quite time-consuming.

Recommended screening of the parotid fossa that optimizes tissue-lesion contrast, lesion detectability, and imaging time is performed by combining a standard T1-weighted acquisition with a T1- or T2-weighted phase-contrast acquisition. Selection of a T1- or T2-weighted phase-contrast acquisition is determined by the T1 characteristics of the lesion.

CT is the established method for cross-sectional imaging of the parotid region. However, MR of this area is currently under investigation by several groups who are employing standard inversion-recovery and spin-echo pulse sequences. Early findings suggest that MR imaging is at least equivalent and perhaps superior to CT in detecting lesions and in distinguishing parotid masses from adjacent structures [1–3]. Because the parotid gland contains a mixture of aliphatic and water protons, MR phase-contrast imaging should provide an additional advantage over standard MR methods, as indicated in recent investigations of other lipid-containing tissues such as the liver and bone marrow [4–8]. We report our initial experience in comparing standard spin-echo imaging with phase-contrast methods, which employed partial-saturation techniques with the MR signal read as a "gradient echo" as well as Dixon's method of chemical-shift imaging.

Phase-Contrast Imaging

A complete description of these techniques is beyond the scope of this report. A comprehensive analysis can be found in the publications of Wismer et al. [7], Dixon [9], Brady et al. [10], and Buxton et al. [11]. The fundamental principle on which these methods is based consists of generating a refocused echo at a time when the transverse magnetization vectors of aliphatic and water protons are 180° out of phase. When this is true, cancellation of the fat and water magnetization vectors occurs. The signal generated is proportional to the absolute value of the signal difference between the two populations of protons. Because most disease processes result in replacement of normal parotid tissue with a predominance of water protons, a region of high signal intensity representing the lesion will be superimposed on a background of low signal intensity representing normal "cancelled" parotid tissue. Tissue-lesion contrast therefore is enhanced.

Chemical-Shift Imaging

The Dixon chemical-shift method uses a standard spin-echo sequence with an alteration in the timing of the 180° pulse with respect to the space-encoding gradients. If $\nu_1 - \nu_2$ is the resonant frequency difference between water and lipid protons, then the earliest time (T) at which they become 180° out of phase is

$$T = \frac{1}{2}\,(1/[\nu_1 - \nu_2]).$$

For a magnet operating at 0.6 T, T is 5.3 msec. The 180° pulse is applied T/2 or 2.66 msec earlier with respect to the read gradient. As a result, the fat and water signals are 180° out of phase during data collection.

The signal generated in a standard spin echo, S_{SE}, from a voxel containing both fat and water is the sum of the fat (S_F) and water (S_W) signals:

$$S_{SE} = S_W + S_F.$$

With the Dixon method, lipid and water proton signals are subtracted in the phase-contrast image,

$$S_{Dixon} = S_W - S_F,$$

where the absolute value is a result of the usual practice of using magnitude reconstructed images. The T1 and T2 relaxation effects are identical in the standard and Dixon sequences.

Gradient-Echo Imaging

In gradient-echo imaging there is no 180° pulse to refocus the effects of differences in resonant frequency due to chemical shift, magnetic susceptibility differences, or B_0 (main magnetic field) inhomogeneities. As a result, the phase difference between the fat and water components of the signal will change with time [12]. Tissues such as the parotid with a significant fat fraction will exhibit a cyclic pattern of signal modulation as the TE is changed and fat and water come in and out of phase at the peak of the echo (Fig. 1). For the simple case of two Lorentzian lines (representing the signal profiles obtained at resonance from fat protons, F, and water protons, W) separated by a chemical shift δ (the difference in resonant frequency between fat and water protons), the magnitude of the gradient-echo signal (S_{GE}) as a function of TE is

$$S_{GE}(TE) = \sqrt{S_W^2 + S_F^2 + 2S_W S_F \cos(2\pi\nu_0\delta TE)}$$
$$S_W = S_{oW}(TR, T1_W, \alpha)\, e^{-TE/T'2_W}$$
$$S_F = S_{oF}(TR, T1_F, \alpha)\, e^{-TE/T2_F^*},$$

where S_{oW} and S_{oF} are the intrinsic water and fat signal intensities that depend on the TR, the respective T1, and the pulse angle α, and ν_0 is the operating frequency of the system. TE thus affects the signal in two ways: (1) decreased signal as TE increases (T2 has been replaced with T2* to indicate the additional effects of B_0 inhomogeneities and magnetic susceptibility variations) and (2) a periodic modulation of the signal between $S_W + S_F$ and $S_W - S_F$ as the phase difference between fat and water evolves. As the field strength increases the signal varies more rapidly with changes in TE. The curve shown in Figure 1 was calculated by fitting this equation to image intensity measurements on the parotid of a normal volunteer (TR = 100 msec and four averages). From this data the fat fraction in the normal parotid parenchyma was 23%. The best-fit curve from the least-squares method yielded a T2* for water of 18 msec, a T2* for fat of 16 msec, and a chemical shift between fat and water resonance of $\delta = 3.44$ ppm.
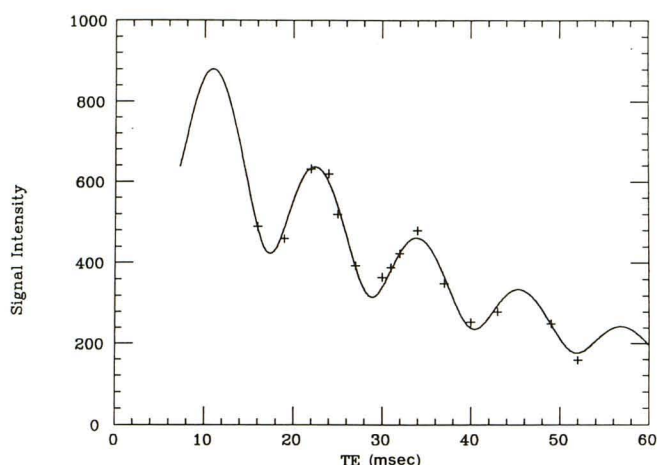

Fig. 1.—Gradient-echo signal intensity vs echo delay (TE). Signal intensity of parotid gland was measured in normal volunteer for various TEs, demonstrating cyclic cancellation of water and fat components by using gradient-echo method with 100-msec TR and four averages. Measured image intensities (+) for TEs between 16 and 52 msec were fit with a simple model line shape consisting of two Lorentzian lines (one for lipid and one for water), with time constants T2-weighted for water (W) and fat (F), separated by a chemical shift (δ). Least-squares fitting produced the best-fit curve shown with the following parameter values: parotid fat fraction = 23%, $T2_W^* = 18$ msec, $T2_F^* = 16$ msec, and $\delta = 3.44$ ppm.
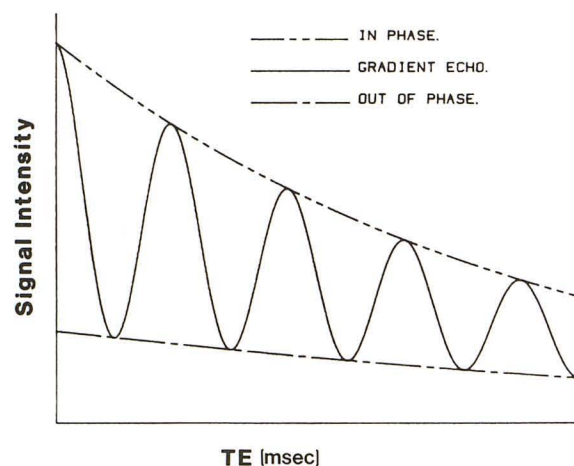

Fig. 2.—Standard and phase-contrast signal intensities vs echo delay (TE). *Out of phase* represents Dixon spin-echo method of chemical-shift imaging, which is independent of TE. This theoretical construct indicates how gradient-echo signal varies as sinusoidal function of TE.

Figure 2 illustrates the standard spin-echo, Dixon spin-echo, and gradient-echo signal intensities as a function of TE. Imaging with either the Dixon or gradient-echo technique becomes arbitrary as long as TE is an integral multiple of time, since both methods will provide similar chemical-shift information (see Discussion).

Subjects and Methods

A series of 10 patients with parotid masses were studied. Imaging was performed on a 0.6-T superconducting system with a 28-cm head coil and 4–5 mm slice thickness. We used a standard multislice and Dixon single-slice spin-echo acquisition, 300–500/20–30/4–6 (TR range/TE range/excitations); a standard multislice acquisition, 2000/

48,96/2–4 (TR/first-echo TE, second-echo TE/excitations); and a single-slice partial-saturation gradient-echo series with four acquisitions: 100/16/4 (90° flip angle), 100/30/4 (20–30° flip angle), 100/50/4 (20–30° flip angle), and 120/100/4 (20–30° flip angle). Altered RF pulse angles were used for the gradient-echo images to either enhance (large flip angles) or suppress (small flip angles) the T1 sensitivity of the pulse sequence [13]. Data in almost all cases were collected on a 256 × 128 matrix. The Dixon sequence was performed with a 2.66-msec shift of the 180° RF pulse. Imaging times were 2.9–5.1 min for the single-slice Dixon sequence, 2.5–9.6 min for the standard multislice T1-weighted spin-echo sequence, 8.5–21.0 min for the standard multislice T2-weighted spin-echo sequence, and 0.9–1.5 min for each single-slice gradient-echo acquisition.

An estimate of tissue-lesion contrast was performed by comparing region-of-interest signal intensity from normal parotid tissue (P), adjacent parotid lesion (L), and background noise (N) measured from a region of interest outside the patient (all regions of measurement greater than 50 voxels). Motion artifact, which in certain instances extended through the parotid into the region outside the patient, was included in the noise measurement. No attempt was made to scale noise for the number of excitations. Tissue-lesion contrast (TLC) was established as

$$TLC = |P - L|/N.$$

This represents a semiquantitative expression of tissue-lesion contrast since comparison is made between standard and phase-contrast methods with similar but not identical imaging parameters such as TR, TE, slice thickness, and number of excitations.

Results

In-phase and out-of-phase acquisitions (Fig. 3) demonstrate the typical phase cancellation that occurs in normal parotid
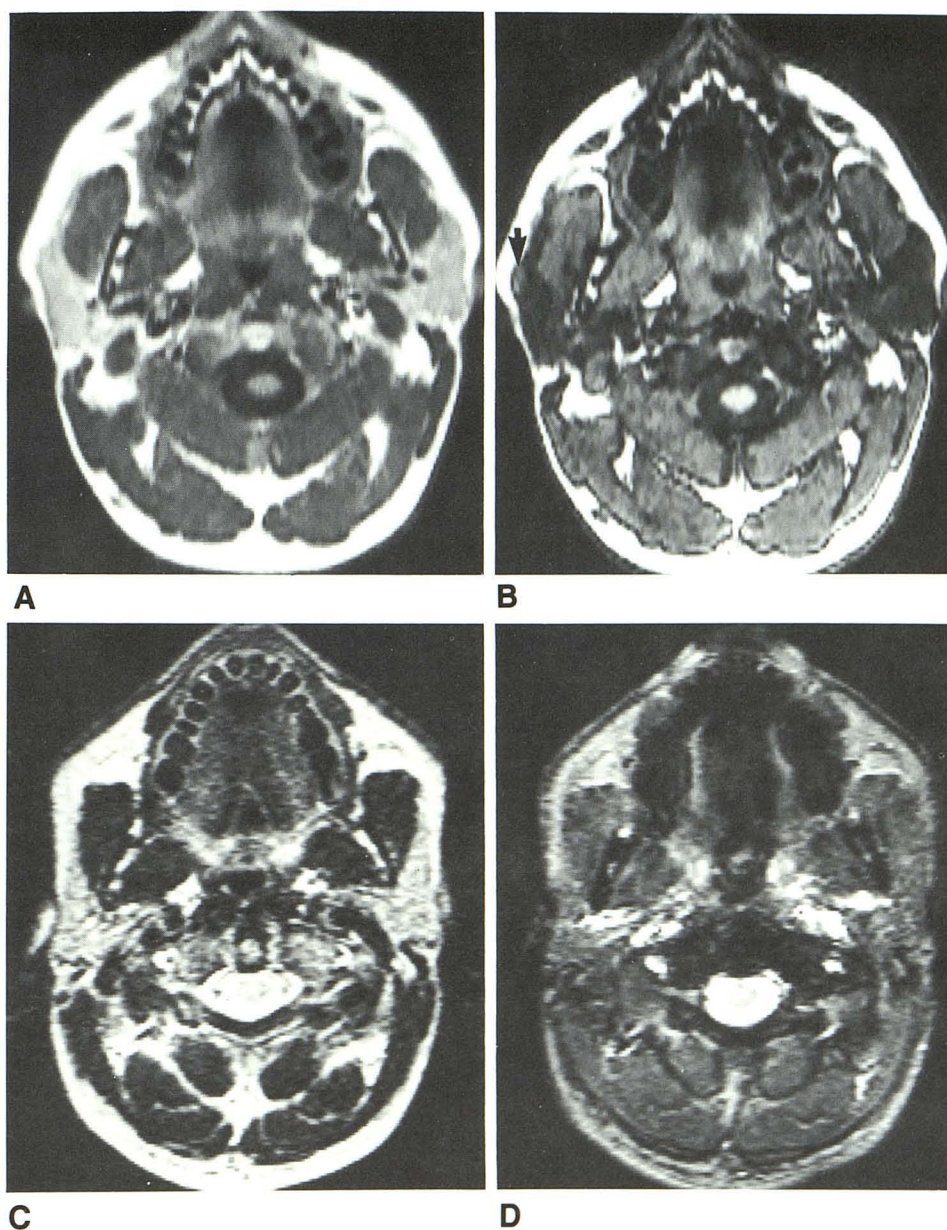

Fig. 3.—Phase cancellation in normal parotid.

A, Standard T1-weighted spin-echo image, 300/25/4.

B, Dixon T1-weighted spin-echo image, 300/25/4. Small periparotid lymph node (arrow) is not seen on standard sequence.

C, Standard T2-weighted spin-echo image, 2000/96/2.

D, T2-weighted gradient-echo image, 100/30/4.

parenchyma with T1- and T2-weighted sequences. A similar reduction in signal occurs at interfaces between subcutaneous fat and those structures with a predominance of water protons; that is, muscle or, more precisely, muscle fascia. This "edge enhancement" is thought to be the result of signal cancellation occurring between aliphatic and water protons, which are separated by a boundary that transects a single voxel.

Table 1 summarizes the imaging characteristics of the 10 patients in this series. MR was positive in 10 of 10 cases and CT was positive in eight of nine cases (CT was not performed in case 3). Contrast-enhanced CT was completely normal in one patient with a palpable mass (case 5). All lesions were detected with standard T1-weighted spin-echo acquisitions, although two lesions (cases 1 and 9) were almost isointense relative to parotid parenchyma. Phase-contrast methods detected nine of 10 lesions, but completely missed the Warthin tumor in case 5. Nevertheless, superior tissue-lesion contrast was obtained in nine of 10 patients with phase-contrast imaging.

Lesions in seven of 10 patients demonstrated both long T1 and long T2. In six of these seven patients, the T2-weighted phase-contrast acquisition provided superior tissue-lesion contrast (a T2-weighted phase-contrast acquisition was not performed in the other patient). Two patients had short T1 lesions. In both cases the T1-weighted phase-contrast acquisition provided superior tissue-lesion contrast.

In view of these findings it can be seen that selection of the phase-contrast method that will provide optimal tissue-lesion contrast can be predicted from the T1 characteristics of the lesion in question.

Representative Case Reports

Case 4

This patient had a long T1/long T2 mixed tumor that was well outlined on the standard T1-weighted spin-echo image (Fig. 4A). The lesion was hyperintense on the standard T2-weighted spin-echo image (Fig. 4B). The T1-weighted phase-contrast acquisition reduced tissue-lesion contrast since the low (long T1) signal generated by the lesion was contrasted against the low signal generated by the phase-cancelled parotid parenchyma (Fig. 4C). The T2-weighted phase-contrast acquisition (Fig. 4D) provided optimal tissue-lesion contrast, confirming the generalization that lesions with long T1 demonstrate superior contrast on T2-weighted phase-contrast acquisitions. Allowing for slight differences in the plane of section, the T2-weighted gradient-echo image was virtually identical to the T2-weighted spin-echo image in appearance and tissue-lesion contrast (14.4 vs 13.5). The main advantage of the T2-weighted gradient-echo image in this instance was speed—1 vs 17 min.

Case 1

A branchial cleft cyst with short T1 and long T2 was T1 isointense and slightly T2 hyperintense relative to normal parotid parenchyma

TABLE 1: Comparison of Standard Spin-Echo and Phase-Contrast Imaging in Parotid Lesions

| Case No.	Age	Gender	Diagnosis	CT	T1	T2	Tissue-Lesion Contrast[a] (Sequence Measured)			
							Standard Spin Echo		Phase Contrast	
							T1-Weighted	T2-Weighted	T1-Weighted[b]	T2-Weighted[c]
1	60	F	Branchial cleft cyst	+	Short	Long	0.1 (300/25/4)	7.3 (2000/96/2)	13.3 (300/25/4)	9.6 (100/30/4)
2	23	F	Mixed tumor	+	Long	Long	4.7 (500/21/6)	3.6 (2000/96/2)	1.7 (300/25/4)	6.1 (100/50/4)
3	46	F	Sjögren disease; cysts	ND	Long	Long	7.8 (300/30/4)	ND	6.1 (300/25/4)	8.7 (100/30/4)
4	36	F	Mixed tumor	+[d]	Long	Long	3.4 (400/21/6)	13.5 (2000/96/4)	3.8 (300/25/4)	14.4 (120/100/4)
5	55	M	Warthin tumor	−	Long	Short	3.0 (300/25/4)	4.5 (2000/48/2)	0.0 (300/25/4)	0.0 (100/30/4)
6	27	F	Branchial cleft cyst	+[d]	Short	Long	3.1 (300/25/4)	2.4 (2000/96/2)	9.9 (300/25/4)	2.5 (100/30/4)
7	67	M	Mucoepidermoid carcinoma	+	Long	Long	9.1 (300/25/4)	0.9 (2000/96/2)	3.3 (300/25/4)	9.4 (100/30/4)
8	13	M	Mixed tumor	+	Long	Long	5.7 (500/21/6)	5.2 (2000/96/4)	3.2 (300/25/4)	10.9 (100/50/4)
9	56	M	Warthin tumor	+	Long	Long	0.6 (500/20/6)	8.2 (2000/96/4)	9.2 (300/25/6)	ND
10	32	F	Mixed tumor	+	Long	Long	3.9 (500/21/4)	3.7 (2000/96/4)	3.5 (300/25/4)	6.3 (100/30/4)

ND = not done.

[a] Tissue-lesion contrast = $|P - L|/N$, where P = parotid signal intensity, L = lesion signal intensity, and N = system noise.

[b] Dixon technique.

[c] Gradient-echo technique.

[d] Nonenhanced CT study was negative.

Fig. 4.—Case 4: mixed tumor.
A, Standard T1-weighted spin-echo image, 400/21/6.
B, Standard T2-weighted spin-echo image, 2000/96/4.
C, Dixon T1-weighted spin-echo image, 300/25/4.
D, T2-weighted gradient-echo image, 100/30/4.
Lesion (*arrows*).
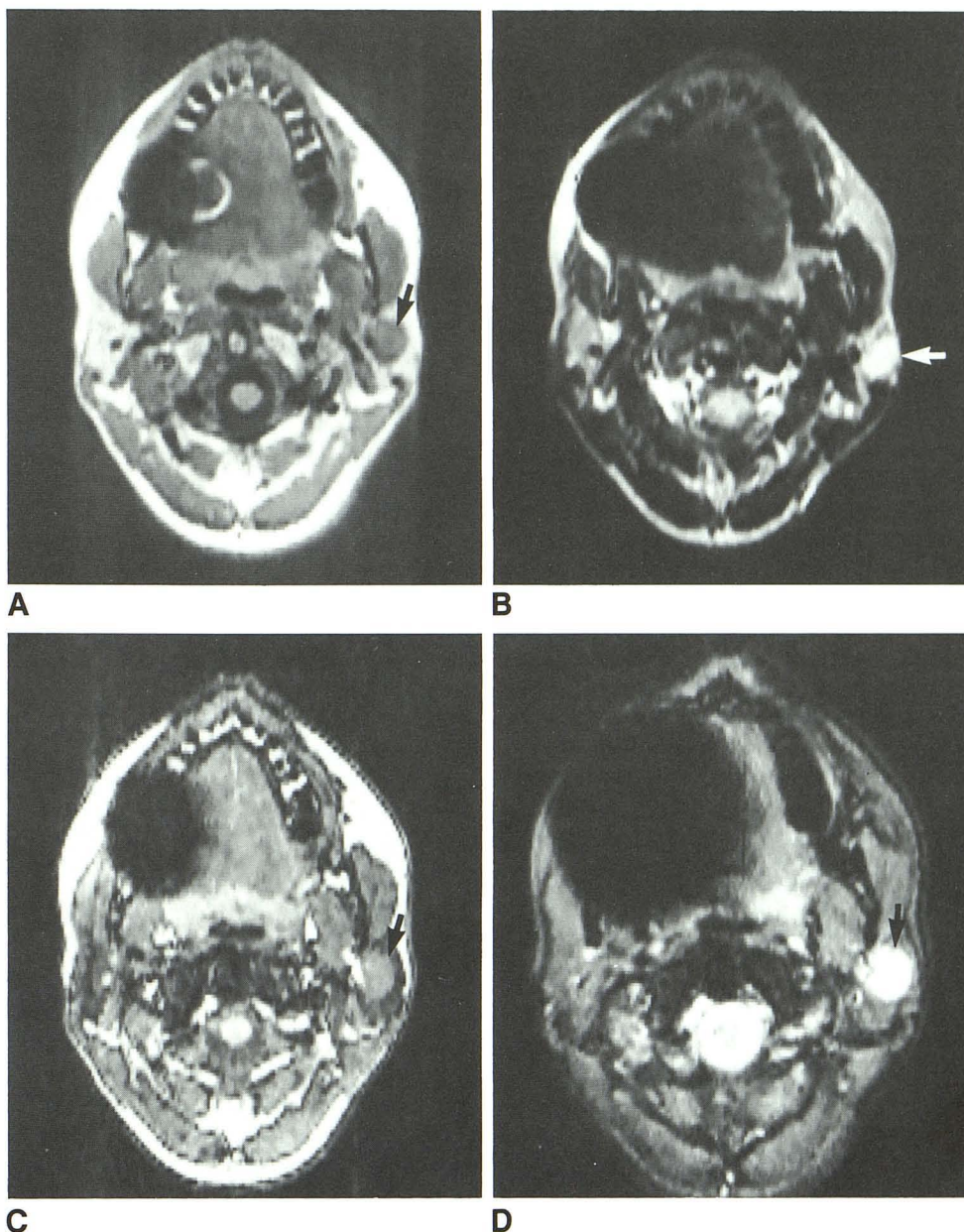
on standard T1- and T2-weighted spin-echo sequences (Figs. 5A and 5B). As expected, the T1-weighted phase-contrast acquisition provided superior tissue-lesion contrast (Fig. 5C). Because the cyst demonstrated long T2 signal, the T2-weighted phase-contrast acquisition provided good tissue-lesion contrast as well (Fig. 5D).

Case 5

This patient had a Warthin tumor that was missed on contrast-enhanced CT because of dental artifact. Standard T1- and T2-weighted spin-echo acquisitions (Figs. 6A and 6B) demonstrated rather unusual signal characteristics with long T1 and short T2. Therefore, the lesion was expected to be difficult to visualize with phase-contrast techniques due to signal loss in the adjacent parotid

parenchyma. As predicted, the lesion was invisible on T1- and T2-weighted phase-contrast acquisitions (Figs. 6C and 6D).

Discussion

In comparing MR with fourth-generation CT in 12 patients with parotid masses, Schaefer et al. [1] considered MR to be equal to or better than CT in parotid imaging with regard to five specific parameters: (1) lesion detection, (2) definition of margins, (3) internal architecture, (4) regional extension, and (5) image degradation secondary to artifact. When contrast-enhanced CT and MR were compared in the 14 cases of Mandelblatt et al. [3], MR provided higher lesion conspicuity
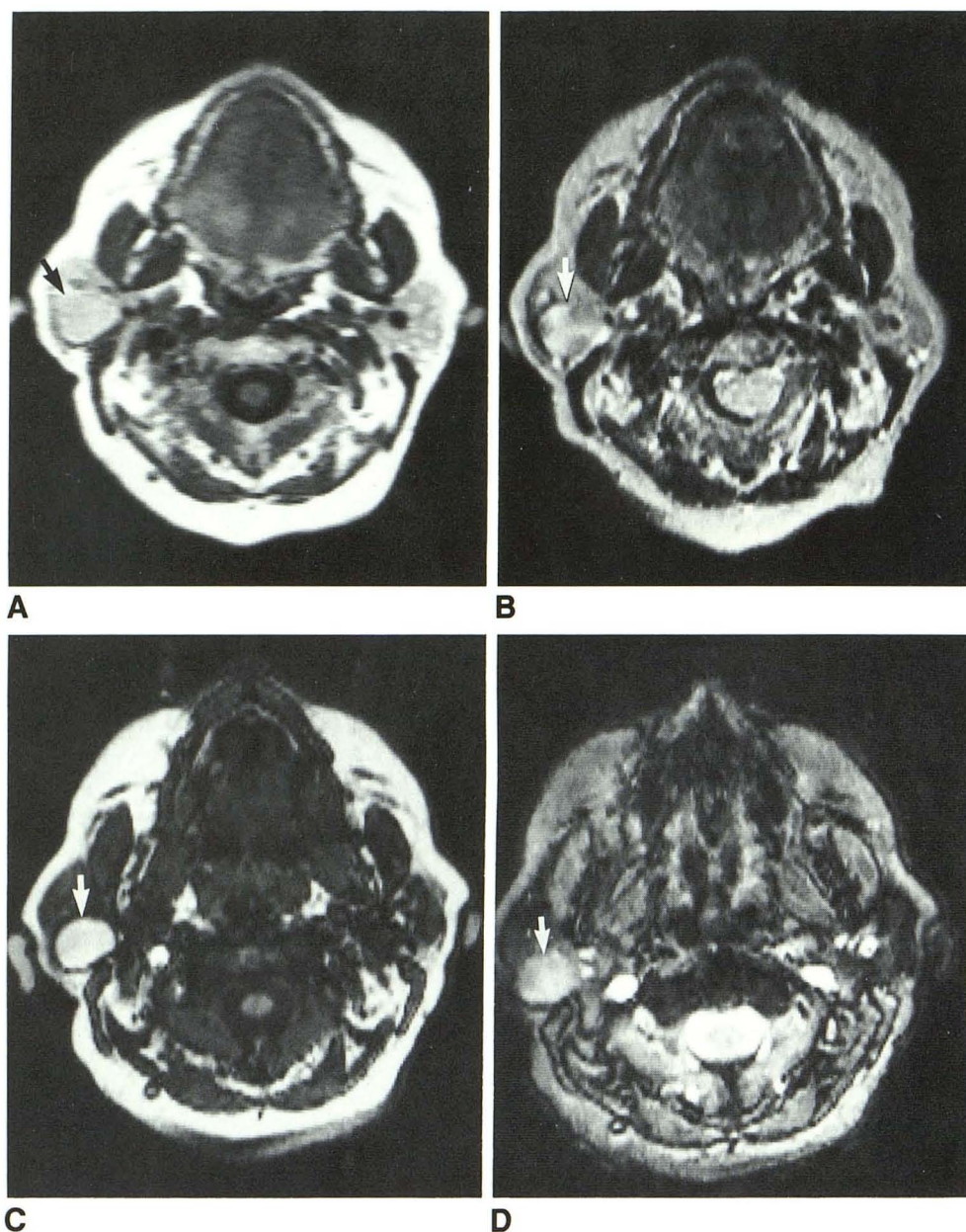
Fig. 5.—Case 1: branchial cleft cyst.
A, Standard T1-weighted spin-echo image, 300/25/4.
B, Standard T2-weighted spin-echo image, 2000/96/2.
C, Dixon T1-weighted spin-echo image, 300/25/4.
D, T2-weighted gradient-echo image, 100/30/4.
Lesion (arrows).

in seven cases, was equal to CT in six, and was inferior to CT in one (due to motion artifact). Teresi et al. [2] were able to distinguish the facial nerve in relation to parotid lesions in nine of 16 patients in whom the nerve was not replaced by tumor. Phase-contrast imaging techniques have been applied to bone marrow [7] and to tumors in the body [8] with obvious benefits in lesion detectability and characterization.

In our series, MR was successful in detecting all parotid lesions and CT was normal in one patient, thus confirming the clinical utility of MR imaging in the parotid region. Furthermore, MR phase-contrast methods offered improved tissue-lesion contrast over standard acquisitions in nine of 10 cases. The single failure occurred as a result of a lesion with

long T1 and short T2, a rarely seen combination of relaxation parameters that matched the phase cancellation in the adjacent normal parotid parenchyma, reducing tissue-lesion contrast to zero.

Choosing between gradient echo and Dixon spin echo to obtain phase-contrast information is influenced by time, line width effects (line broadening), and scanner flexibility. The gradient echo is faster than the spin echo, but the spin echo offers higher signal to noise since it is not susceptible to T2* effects, which result in broadening of the proton resonant frequency distribution (line width effects), reducing the intensity of the gradient-echo signal. Errors in the value of the chemical shift δ used to obtain timing parameters for appli-

Fig. 6.—Case 5: Warthin tumor.
A, Standard T1-weighted spin-echo image, 300/25/4.
B, Standard T2-weighted spin-echo image, 2000/48/2.
C, Dixon T1-weighted spin-echo image, 300/25/4.
D, T2-weighted gradient-echo image, 100/50/4.
Lesion (*arrows*).
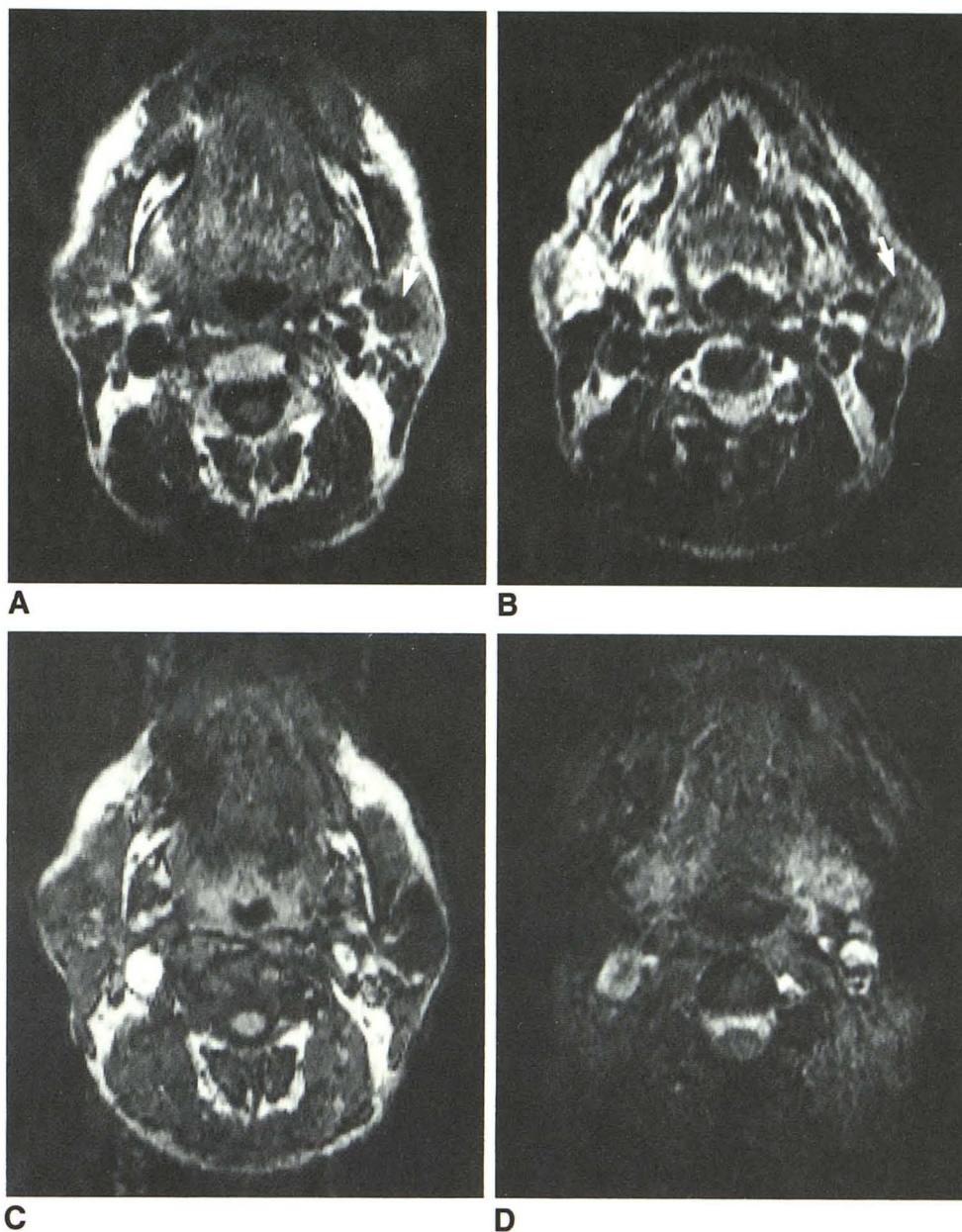
cation of the spin-echo 180° pulse and application of the gradients in the gradient echo will result in echoes occurring at a time when fat and water protons are not exactly 180° out of phase. The gradient echo is more sensitive to this effect than the spin echo, since the phase error accumulates over a time (T) equal to the TE, whereas the time of accumulation of the phase error with the spin echo is equal to 5.3 msec (T = 5.3 msec at 0.6 T). Phase errors can be eliminated with the gradient-echo method by obtaining empirical data of signal intensity vs TE, as we did in Figure 1 to determine the TEs that result in maximum signal cancellation. Finally, scanner characteristics may impose limitations on whether a gradient echo or spin echo can be obtained with chemical-shift

information because hardware and software features may or may not allow the necessary pulse sequence modifications.

With regard to imaging parameters, the following values were found to be most useful: (1) standard and Dixon T1-weighted spin echo, 400/20/4, and (2) standard T2-weighted spin echo, 2000/48,96/4. For gradient-echo imaging, chemical-shift information is dependent only on TE and is independent of flip angle. From Figure 1, maximal chemical-shift information will be present at TEs of 18, 29, and 41 msec, etc. Gradient-echo T1 and T2 weighting is dependent on both TE and flip angle. T1 weighting is obtained with short TEs and large flip angles, whereas the opposite is true for T2 weighting. Considering these factors, the following parameters pro-

TABLE 2: Phase-Contrast Selection Criteria for Parotid Tumors

T1 Signal of Parotid Lesion	Phase-Contrast Acquisition
Long	T2-weighted
Isointense	T1- ± T2-weighted
Short	T1-weighted

vide the desired results at 0.6 T: (1) T1-weighted gradient echo, 100/18/4 (90° flip angle), and (2) T2-weighted gradient echo, 100/29/4 (30° flip angle).

The goals of MR imaging of the parotid fossa are (1) lesion detection, (2) optimization of tissue-lesion contrast, and (3) reduction of overall imaging time. Lesion detection is maximized through use of both standard and phase-contrast techniques since the latter can discriminate lesions that are isointense relative to normal parotid parenchyma on standard imaging. Optimal tissue-lesion contrast is usually, but not exclusively, obtained with phase-contrast acquisitions. Reduction of imaging time is achieved through the use of T2-weighted gradient-echo acquisitions, which can reduce T2 imaging times by approximately 90%.

We recommend the following imaging strategy to achieve these goals. The parotid should be screened initially with a standard T1-weighted spin-echo sequence since lesion detectability and tissue-lesion contrast are usually good. If optimization of tissue-lesion contrast is desired, then selection of the phase-contrast acquisition that will provide this result can be based on the T1 signal characteristics of the lesion as seen on the initial T1-weighted screening acquisition, according to Table 2. If the lesion demonstrates a long T1, then a T2-weighted phase-contrast acquisition will optimize tissue-lesion contrast. For short T1 lesions, T1-weighted phase-contrast acquisitions will provide superior tissue-lesion contrast. If no lesion is detected on the screening sequence (i.e., the lesion is isointense), then a T1-weighted phase-contrast acquisition should provide optimal tissue-lesion contrast. T2-weighted phase-contrast sequences can be performed as needed to obtain T2-weighted information in place of standard T2-weighted spin-echo acquisitions.

Our preliminary experience indicates that phase-contrast imaging of the parotid region can optimize tissue-lesion contrast in the majority of parotid lesions and therefore serves as a useful adjunct to standard spin-echo imaging. Furthermore, the time required to obtain T2-weighted information can be sharply reduced with the gradient-echo method.

REFERENCES

1. Schaefer SD, Maravilla KR, Close LG, Burns DK, Merkel MA, Suss RA. Evaluation of NMR versus CT for parotid masses: a preliminary report. *Laryngoscope* **1985**;95:945–950
2. Teresi LM, Lufkin RB, Wortham DG, Abemayor E, Hanafee WN. Parotid masses: MR imaging. *Radiology* **1987**;163:405–409
3. Mandelblatt SM, Braun IF, Davis PC, Fry SM, Jacobs LH, Hoffman JC. Parotid masses: MR imaging. *Radiology* **1987**;163:411–414
4. Lee JKT, Heiken JP, Dixon WT. Hepatic metastases studied with MR and CT. *Radiology* **1985**;156:423–427
5. Lee JKT, Heiken JP, Dixon WT. Detection of hepatic metastases by proton spectroscopic imaging. *Radiology* **1985**;156:429–433
6. Stark DD, Wittenberg J, Middleton MS, Ferrucci JT Jr. Liver metastasis: detection by phase-contrast MR imaging. *Radiology* **1986**;158:327–332
7. Wismer GL, Rosen BR, Buxton R, Stark DD, Brady TJ. Chemical shift imaging of bone marrow: preliminary experience. *AJR* **1985**;145:1031–1037
8. Paling MR, Brookeman JR, Mugler JP. Tumor detection with phase-contrast imaging: an evaluation of clinical potential. *Radiology* **1987**;162:199–203
9. Dixon WT. Simple proton spectroscopic imaging. *Radiology* **1984**;153:189–194
10. Brady TJ, Wismer GL, Buxton RB, Stark DD, Rosen BR. Magnetic resonance chemical shift imaging. In: Dressel HY, ed. *Magnetic Resonance Annual*. New York: Raven Press, **1986**;55–80
11. Buxton RB, Wismer GL, Brady TF, Rosen BR. Quantitative proton chemical shift imaging. *Magn Reson Med* **1986**;3:881–900
12. Wehrli FW, Perkins TG, Shimakawa A, Roberts F. Chemical shift-induced amplitude modulations in images obtained with gradient refocusing. *Magn Reson Imaging* **1987**;5:157–158
13. Buxton RB, Edelman RR, Rosen BR, Wismer GL, Brady TJ. Contrast in rapid MR imaging: T$_1$- and T$_2$-weighted imaging. *J Comput Assist Tomogr* **1987**;11:7–16